

Integrating seismic attributes and rock physics for delineating Pliocene reservoir in Disouq field, Nile Delta, Egypt

Ahmed HESHAM* , Nadia Abdel FATTAH , Aia DAHROUG 

Geophysics Department, Faculty of Science, Cairo University, Giza, Egypt

Abstract: The Nile Delta is known as the most prolific gas province in North Africa. Gas exploration and production were the main targets over decades in the Nile Delta. The integration of petrophysical analysis, seismic interpretation, and seismic attributes could indicate the presence of gas in Disouq field, which is located in Nile Delta, Egypt. Well log data showed that the reservoir is classified into three zones (A, B, and C). These zones are characterized by low gamma ray (around 35%), with relatively high porosity (around 29%) and low water saturation (36–38%). Structural and stratigraphic interpretation was conducted in order to investigate the extension and geometry of the reservoir, in addition to the faults affecting the study area. The reservoir is represented by a channel of Pliocene age, characterized by the low impedance sand saturated by gas. Near and far offset data show the gas effect. There is an increase of the negative amplitude from near to far offset. The amplitude map and structural contours match well and show good conformance. Seismic attributes including surface attributes and “Red Green Blue/colour blending” help in delineating the extent and geometry of the reservoir, in addition to the possible prospect. Finally, the volume of original gas in place was estimated what showed that the study area is of great economic interest.

Key words: Nile Delta, Pliocene reservoir, seismic interpretation, seismic attributes, calibrated check shot, Disouq field

1. Introduction

The Nile Delta represents a prolific North African gas province. In addition to its agricultural and population potentialities (*Dolson et al., 2001*), it represents one of the main petroleum provinces in Egypt (*Dolson et al., 2001*). It is well known for its recent onshore and offshore gas discoveries. The Disouq concession (displayed with geographic coordinate system) (Fig. 1) is located on the onshore part of the Delta. It spreads over an area of 5,523 km² and the “North Sidi Ghazy” gas discovery is the main asset of this concession.

*corresponding author, e-mail: geo.a.hesham@hotmail.com

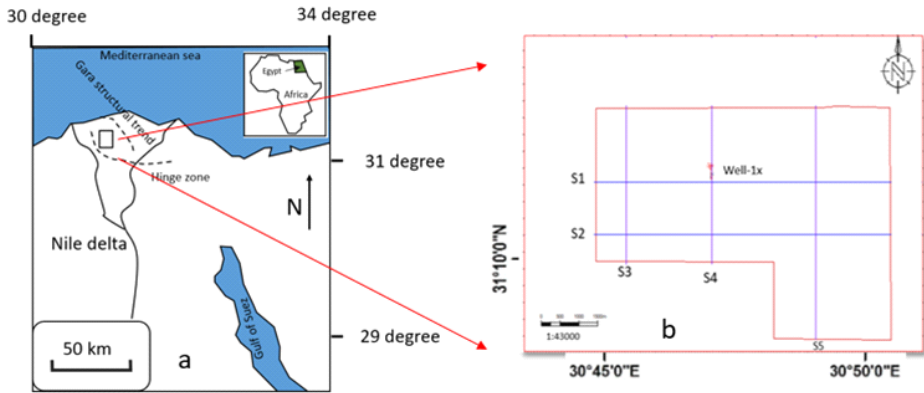


Fig. 1. The Nile delta in Egypt (a) (modified after *Younes, 2015*); the study area (b).

The main objectives of this study include tracing the possible prospect and leads for hydrocarbon reservoir zones; in addition, this work aims to estimating the volume of original gas in place. Moreover, mapping top El Wastani and the top of Kafr El Sheikh Formations will be performed.

2. Geological settings

2.1. Lithostratigraphy

The Cretaceous-Miocene rocks have been drilled in the sub-stratum of the Nile delta and are exposed in the Western Desert fringes (*Kellner et al., 2009*). The lithostratigraphy of the delta is classified as follows (*Kamel et al., 1998*) Moghra, Sidi Salem and Abu Madi formations (Miocene to Pliocene; Fig. 2). The delta body consists mainly of sand and clays that were deposited by fluvial activity during the Pliocene-Quaternary time. The Plio-Pleistocene sequences are mainly represented by shale or clay with sandstone interbeds (Fig. 2). The Holocene silty and clay layer increase in thickness northward and cap these deposits. Particularly toward offshore the mentioned intervals contain several sand lenses and sand wedges (*Said, 1990*). The study focusses on two formations:

- 1) The Kafr El Sheikh Formation (lower-middle Pliocene) which consists of mudstone sequence with thin limestone and sandstone interbeds. This formation extends all over the Delta area. *Rizzini et al. (1978)* suggested

that the Kafr El Sheikh Formation represents neritic mudstones, which represents the onshore zone of the delta and pass into basinal offshore mudstones. It was suggested that the sands incorporated into this formation are essentially tempestite beds. This formation is conformably overlain by El Wastani Formation (*Kamel et al., 1998*).

- 2) The El Wastani Formation (upper Pliocene) consists of thick sand beds interbedded with thin clay beds, which become thinner toward the top of the formation. The formation is transitional between shelf facies of the underlying Kafr El Sheikh Formation and coastal to continental sands of the overlying Mit Ghamr Formation (Pliocene-Holocene; *Kamel et al., 1998*).

AGE	STAGE	FORMATION	LITHOLOGY	DISCOVERIES
HOLOCENE	MILAZZIAN	BILQAS MIT GHAMR		
PLESITOCENE	SICILIAN			
	CALABRIAN	EL WASTANI		★
PLIOCENE	PIACENZIAN	KAFR EL SHEIKH		★
	ZANCLEAN			▲
MIOCENE	MESSINIAN	ABU MADI		★
	TORTONIAN	QAWASIM		●
	SERRAVALLIAN	SIDI SALEM		●
	LANGHIAN			●
	BURDIGALIAN	QANTARA		●
	AQUITANAIN			▲
OLIGOCENE	CHATTIAN	TINEH		▲

	SANDSTONE		EVAPORITES
	SHALE-CLAY	★	GAS
▲	SOURCE	●	OIL & GAS

Fig. 2. Stratigraphic succession of the Nile delta (modified after *Kamel et al., 1998*).

2.2. Structural settings

The structural elements affecting the northern margin of Egypt, including the Nile Delta, were formed during the tectonic evolution (5.9 million years

ago) of the southern part of Eastern Mediterranean basin (*Garfunkel, 1998; Guiraud and Bosworth, 1999; Abdel Aal et al., 2001; Abd-Allah, 2008*). This region represents the Northeast African continental margin that is covered by deltaic sediments. Structurally, the Plio-Pleistocene sediments of the Nile Delta are dissected by the East–West, North–South, northwest (Temsah trend), and northeast (Rosetta trend) striking faults (*Harms and Wray, 1990; Sarhan and Hemdan, 1994; Abdel Aal et al., 1994; Sarhan et al., 1996*). The northwest and northeast oriented faults dissect mainly the northeastern and northwestern margins of the delta, respectively. The northwest and northeast oriented faults intersect together at the southern boundary of the Messinian salt basin, in the central Mediterranean Sea (*Abdel Aal et al., 2001*). The onshore part of the delta is affected by several East–West trending fault systems that extend into the other regions (e.g. fields around Damietta branches in Nile delta) of Northeast Egypt (e.g. *Sestini, 1984; Moustafa et al., 1998; Hussein and Abd-Allah, 2001; Abd-Allah, 2008*). The Nile Delta is characterized by asymmetric fold, overthrust faults and salt diapirs. It dates back to the Syrian Arc system (Upper Cretaceous) which has an arcuate trend from northeast to southwest through the northern part of the Nile Delta to the Western Desert of Egypt (*Abdel Aal et al., 2001*).

3. Data and methods

Seismic and petrophysical data were integrated in order to calculate the volume of original gas in place. The seismic data is comprised of five 2D seismic lines (near and far offset data). The near offset data ranges from zero to 15 degree, while the far offset data ranges from 30 to 45 degree. The seismic sections were utilized to map and trace the top of El Wastani and Kafr El Sheikh Formations in addition to other Pliocene levels.

In this study, 2D arbitrary seismic lines were extracted from a 3D cube. The seismic data was tied to a key well (Well-1X) that includes multiple well log curves namely: gamma ray, resistivity, density, neutron and sonic logs. The surface attribute was extracted to show the geometry of the reservoir as well as the potentiality of hydrocarbon, while the colour blending technique has been applied in order to investigate the promising area. This has been conducted by using Petrel software.

3.1. Workflow

The work starts with investigating the petrophysical evaluation of well 1X. Second, synthetic seismogram was generated in order to perform seismic to well tie. Seismic interpretation followed. Third, a velocity model was created to perform depth conversion. Fourth, surface attribute and colour blending were utilized to highlight the promising area. Finally, the volume of original gas in place was estimated.

3.2. Log interpretation and petrophysical analysis

Rock properties are the physical properties of rocks that influence the propagation of seismic waves. They basically include compressional wave velocity, shear wave velocity, density and their numerous derived attributes which include P-wave impedance, Poisson's ratio, S-wave impedance, etc. (Dewar, 2001). The observed amplitudes on seismic data represent contrast or variation in these rock properties at the boundary between two geological or geophysical interfaces, i.e., changes in lithology or fluid in the subsurface (Brown, 1987). In this study, Well-1X has encountered several reservoir rocks which were displayed and interpreted in the Petrel software (Fig. 3).

Water saturation is calculated by Archie equation (Archie, 1952):

$$S_w^n = \frac{a R_w}{\phi^m R_t}, \quad (1)$$

where S_w : water saturation (percentage), n : cementation exponent (unitless), a : tortuosity factor (usually one), ϕ : porosity(percentage), R_w : water resistivity in Ohm.m, R_t : true resistivity in Ohm.m.

Gamma ray and resistivity logs helped in determining the three zones. Archie equation was used to calculate petrophysical parameters of these three zones within reservoir (Table 1).

Table 1. Petrophysical paramters for three intervals in Pliocene reservoirs in the Well-1X (Suez, 2014).

zones	average effective porosity	av. S_w	net pay	gross	net/gross
A	29.5	48	2.1	16.8	0.125
B	30	36	8.8	12.2	0.72
C	29.6	38.9	12.8	18.9	0.67

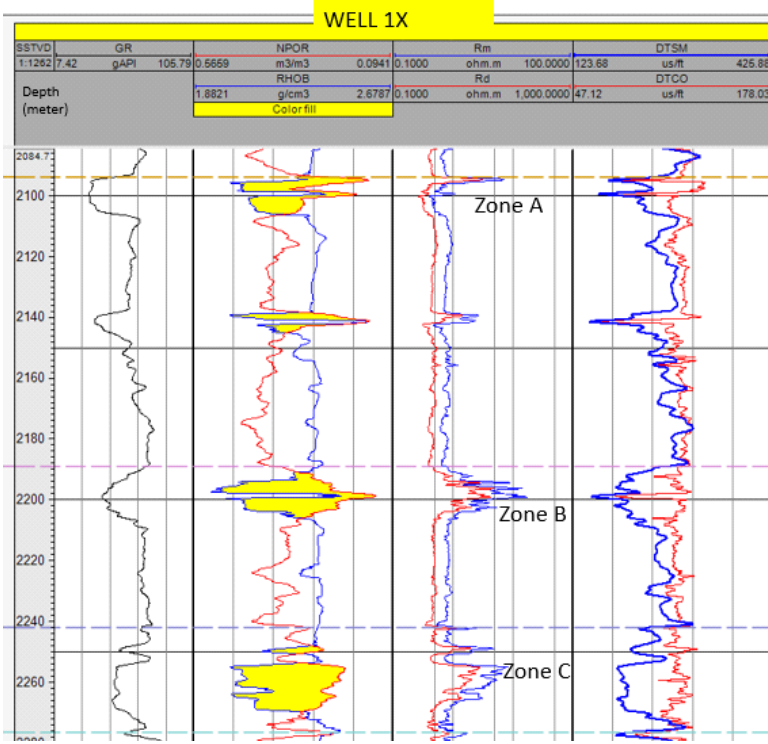


Fig 3. Petrophysical logs for Well-1X in zones A, B.

3.3. Clay volume analysis

The clay volume interpretation analysis is used to interactively calculate volume curves from gamma ray. The interpretation problem in fine grained formations is the calculation of porosity and saturation values free from the shale effect because the shale effect depends on the shale content; the estimation of the volume of shale content is of prime importance (Suez, 2014).

Qualitatively, the volume of shale content indicates whether the Formation can be considered clean or shaly. This determines the types of the model or approach to be use in the interpretation. Quantitatively, the volume of shale content is used to estimate the shale effect on log responses and to correct them to the clean Formation responses (Schlumberger, 1987). In this study, the gamma ray log is used as the Single Clay Volume Indicator.

Shale content can be calculated using the following equation (*Schlumberger, 1987*):

$$V_{sh} = \frac{GR_{\log} - GR_{\min}}{GR_{\max} - GR_{\min}}, \quad (2)$$

where V_{sh} is the shale content, GR_{\log} is the gamma ray reading of the analysed zone, GR_{\min} is the minimum gamma ray reading in front of clean sand, GR_{\max} is the maximum gamma ray reading in front of a shale bed (*Schlumberger, 1987*).

3.4. Cut-off and summations

The cut-off and summation help in defining the net reservoir and net pay. The input data to assign the cut-off values include effective porosity, clay volume and water saturation. These values are critical in calculating the petrophysical parameters (Table 2), which will be consequently used to determine the original gas in place.

Table 2. Cut-off values (*Suez, 2014*).

cut-off value		
effective porosity (%)	water saturation (%)	volume of clay (%)
0.1	0.65	0.36

3.5. Seismic to well tie

The Well-1X was conducted as combined zero offset and walk above VSP (vertical seismic profile). A vibrator was used as a static source and was located 85m from the wellhead and explosives were used in a walk-above survey to gather data at 130 levels from the deviated part of the well. Generally, each shot allowed for one level overlap to the previous shot (*Suez, 2014*).

The seismic wavelet is the link between seismic data (traces) on which interpretations are based and the geology (reflection coefficients), and it must be known to interpret the geology correctly. However, it is typically unknown, and assumed to be both broad band and zero phases. Providing this broad band, zero phase wavelet is the processing goal of deconvolution. Unfortunately, this goal is rarely met and the typical wavelet that remains

in fully processed seismic data is mixed-phase (*Henry, 1997*).

Deterministic wavelet was extracted from surface seismic and this extraction was performed along well path deviation. The frequency ranges from 25 Hz to 55 Hz. The reflection coefficient was generated by sonic and density logs, in addition to the check shot. Finally, the synthetic seismogram was formed and the correlation factor after adjustment is set to 0.73 (Fig. 4).

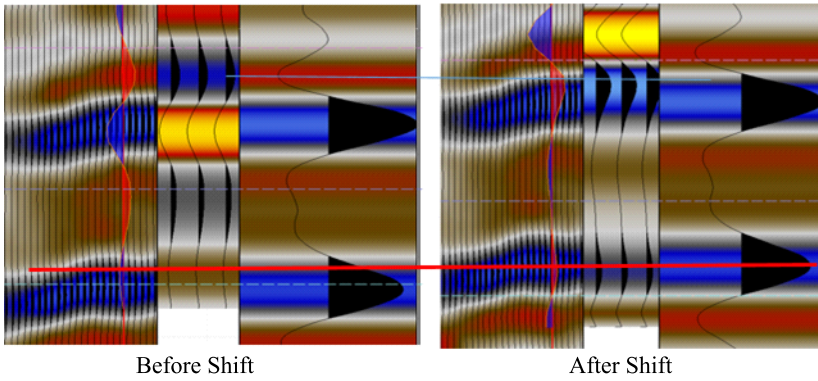


Fig. 4. Synthetic seismogram of Well-1X before and after shift.

3.6. Seismic interpretation

The seismic reflection data used in this study consists of five processed seismic profiles covering the study area. Well-1X was tied to the seismic grid. One of the main principles of seismic interpretation is to identify the important seismic reflectors that represent lithological and stratigraphical boundaries, in addition to identify the subsurface structures affecting these reflectors (*Van Wagoner et al., 1987*). The resolution of the seismic volume in vertical and lateral directions varies from barely good to poor in some sections based on the resolution it deteriorates with increasing depth. Therefore, the vertical seismic profile was conducted, in order to accurately identify the formation tops and generate depth structure maps of the picked strata.

The important reflectors are picked on the basis of well markers as the resolution of seismic is moderate and the picked reflectors should be tied together around the grid of the seismic lines (looped process).

El Wastani and Kafr El Sheikh reservoirs were mapped using near angle stacks data since near data is closer to lithology while far offset data are used to show fluid effect. The reservoir is represented by a channel of Pliocene within El Wastani formation. This reservoir channel isn't influenced by faults but it is sealed by a shale layer, while Kafr El Sheikh Formation is affected by normal fault. This fault has N–S trend with great throw reaching up to 175 meters. Two seismic lines were selected as an example to delineate the Pliocene channel (Figs. 5, 6).

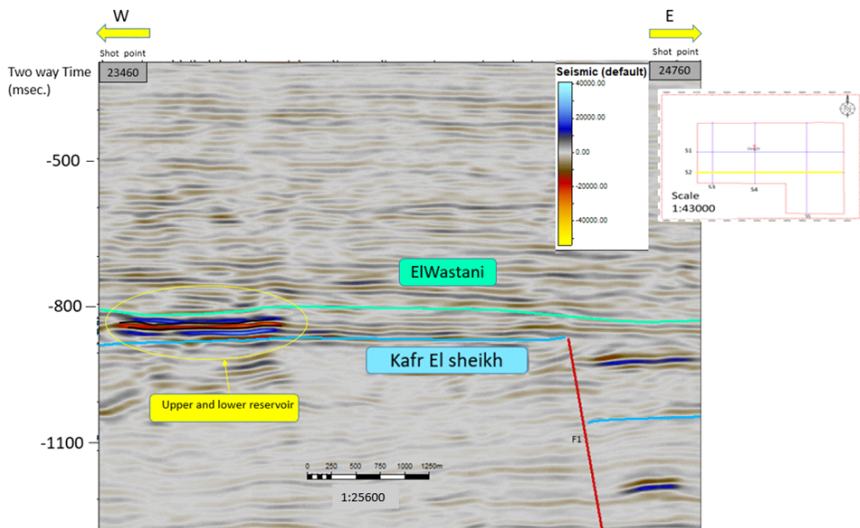


Fig. 5. Interpreted seismic section (S2) illustrates distribution and levelling of El Wastani and Kafr El Sheikh Fms.

After the interpretation of seismic sections, a TWT map is generated for the upper geobody, which belongs to El Wastani reservoir (Fig. 7).

3.7. Velocity modelling

Velocity modelling (Fig. 8) is generated to perform the conversion from time maps to depth. Top model is generated as constant surface at zero seconds. Velocity maps of El Wastani Fm. and Kafr El Sheikh Fm are generated and controlled by the well data. Base model is generated as constant surface at 3 second to cover most of the data.

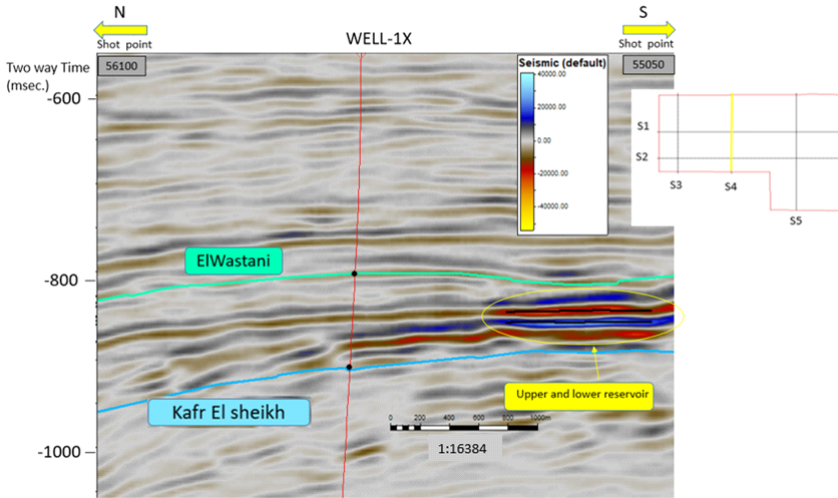


Fig. 6. Interpreted seismic section (S4) illustrates distribution of El Wastani and Kafr El Sheikh together with the distribution of Pliocene reservoir.

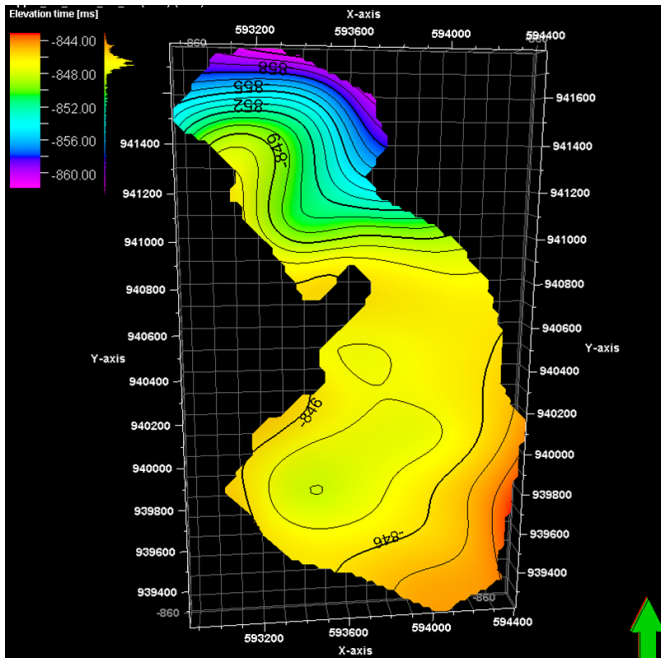


Fig. 7. Two-way time map of the upper Pliocene channel (reservoir).

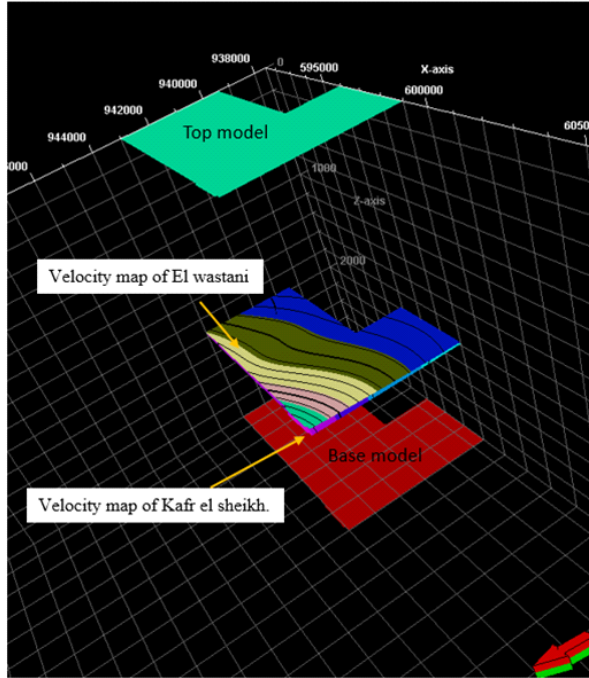


Fig. 8. Velocity modelling.

After examination of the velocity maps, we can conclude that there is no large heterogenic velocity.

3.8. Depth structure map

The main formula of velocity (*Newton, 1687*):

$$Velocity = \frac{Z}{OWT}, \tag{3}$$

where Z is the depth of a certain layer and OWT is one-way time of the traveling wave.

So the depth-converted maps is generated by using velocity model and time maps. Depth map is generated for the upper Pliocene levels (Fig. 9).

Geological cross section has been created to illustrate the geometry of the Pliocene channel (Fig. 10). It is composed of sandstones sealed by a shale formation. The charge enters the channel from the south and progrades

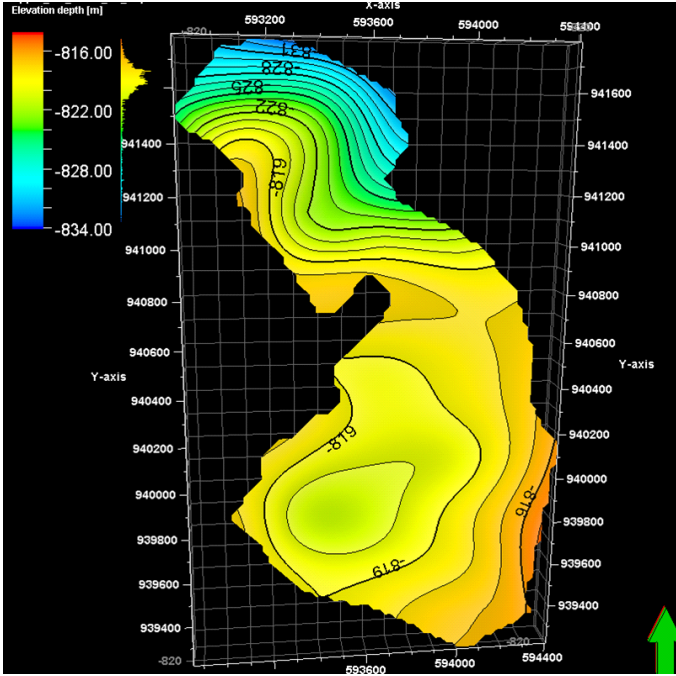


Fig. 9. Depth converted map of the upper Pliocene reservoir channel.



Fig. 10. Geological cross section along the channel (a); map showing the direction of section (b).

towards the north. Sealing is provided by a shale formation. The channel thickness is ranging from 10 m to 18 m.

3.9. Surface attributes map

The first use of amplitude information as hydrocarbon indicators was done in the early 1970s when it was found that bright-spot amplitude anomalies could be associated with hydrocarbon traps (*Hammond, 1974*). The sum of negative amplitude was extracted as surface seismic attribute to indicate the presence of gas. The hydrocarbon bearing zone is characterized by low impedance and could successfully be indicated by using this attribute. This attribute was extracted by using the top horizon of the Pliocene channel with $[-5, +5]$ millisecond window above and below the Pliocene horizon. As it is illustrated (Fig. 11), there is an increase in the sum of negative amplitude from near to far offset which points to presence of gas.

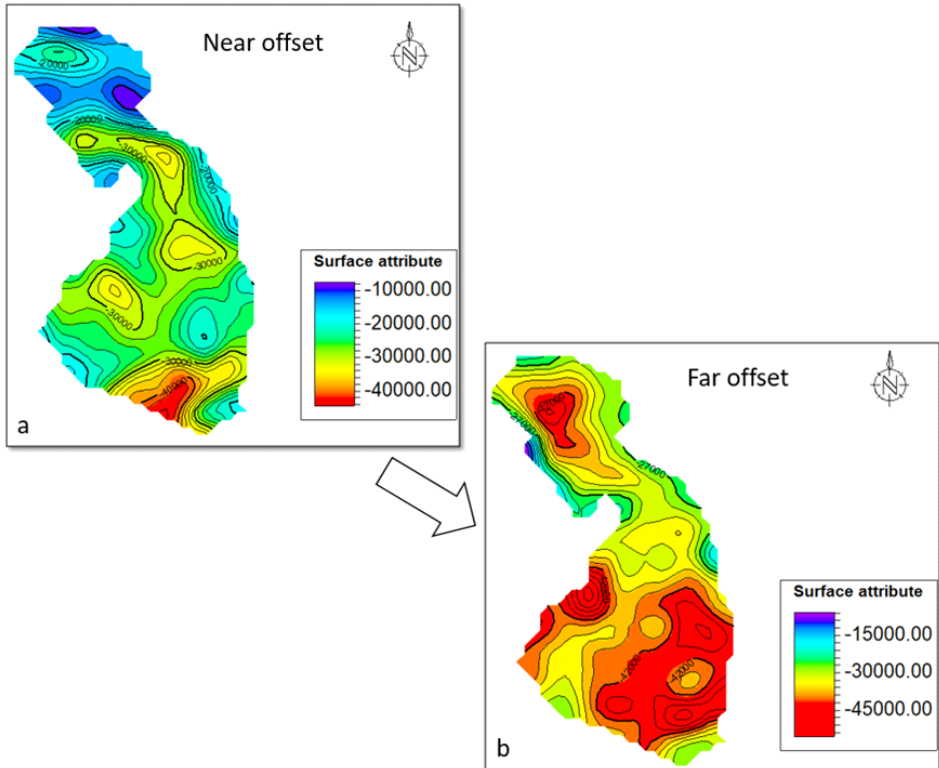


Fig. 11. Sum of negative amplitude at near (a) and far (b) offset.

3.10. RGB colour blending

Colour always plays a key role in seismic attribute analysis. It is very powerful tool, which is used to represent data and give interpreter visual elaborations. Due to the development of hardware capabilities, 3D visualization has become a core component of seismic interpretation workflows (Cao *et. al.*, 2015).

Standard Frequency Decomposition extracts band-limited versions of the data and offers a much more sensitive method of analysing seismic data than the full frequency amplitude response. It can provide information about stratigraphic facies boundaries, structural and stratigraphic geometries, stratigraphic heterogeneity and bed thickness. When three frequency magnitude responses are combined in a RGB (Red-Green-Blue) colour blend, the relationships and interplay between the frequency responses can be investigated. Standard Frequency Decomposition and RGB Blending workflow has many procedures (Henderson *et al.*, 2007) as will be discussed in detail below.

First, the spectral analysis has been performed to determine the bandwidth and dominant frequency. Secondly, spectral decomposition for far offset data at three frequencies 12, 29, 46 Hz was done. These three frequencies are selected from the frequency spectrum as the minimum and maximum. Frequency represents the start and the end plateau of the spectrum. Finally, applying colour blending for these three frequencies is performed.

The time slice at eight hundred and sixty milliseconds has been generated to illustrate the effect of colour blending in the Pliocene level (Fig. 12).

4. Results

4.1. The original gas in place (OGIIP)

The original gas in place has been calculated (Eq. (4)) by using many parameters like the area and thickness of reservoir, porosity, water saturation and gas formation volume factor with using some parameters from Table 1.

$$G = 43560 A h \phi \frac{(1 - S_{wi})}{B_{gi}}, \quad (\text{Ahmed, 2010}) \quad (4)$$

where G = gas-in-place (scf), A = area of reservoir (acres), h = average

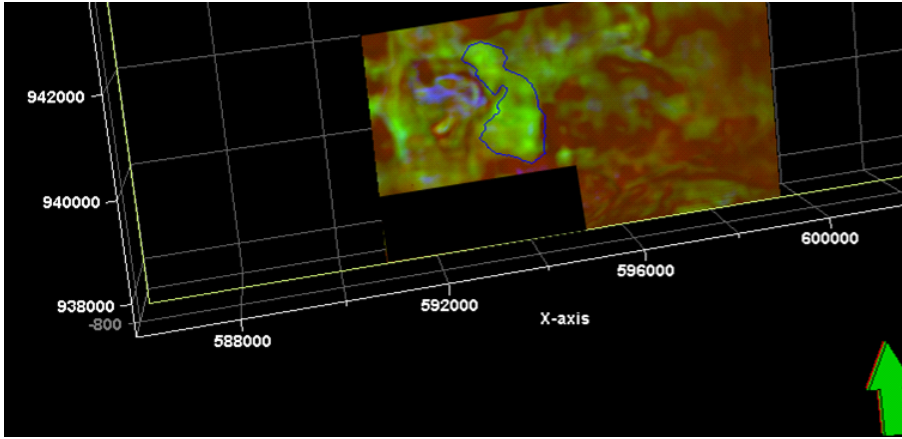


Fig. 12. Time slice of colour blending at 860 ms (two-way time). This time slice represents the blending of three frequencies and the dominant frequency is represented by the green colour, this is why the green colour is most pronounced than the others.

reservoir thickness (ft), ϕ = porosity, S_{wi} = water saturation, and B_{gi} = gas formation volume factor (ft³/scf, standard cubic feet).

Gas formation volume factor B_g (Eq. (5)) is defined as the actual volume occupied by n moles of gas at a specified pressure and temperature, divided by the volume occupied by the same amount of gas at standard conditions. Applying the real gas equation-of-state to both conditions gives:

$$B_g = 0.02827 \frac{Z T}{P}, \quad (\text{Ahmed, 2010}) \tag{5}$$

where B_g = gas formation volume factor (ft³/scf), Z = gas compressibility factor, T = temperature (°R), P = specified pressure (Psi).

By applying the previous equation with the following parameters as recorded from the well (Table 3) the value of gas formation volume factor takes the value 0.004532 ft³/scf.

Table 3. The parameters for calculating gas formation volume factor.

Z	temperature (°R)	P (PSI)
0.998	655	4079

Three cases have been estimated to shows the maximum case (P90) and the minimum case (P10) and the most probable case (P50) from the three

zones in Well-1X (Table 4).

Table 4. Different petrophysical parameters for calculating original gas in place in three different cases.

probability	av. porosity (%)	av. saturation (%)	net/gross
P10	29.5	48	0.125
P50	29.6	39	0.67
P90	30	36	0.72

After using the previous parameters (Table 4) and substituting Eq. (5) in Eq. (4), original gas in place (Bscf – billion standard cubic feet) has been calculated in three scenarios (Table 5).

Table 5. Original gas in place with three scenarios.

probability	P10	P50	P90
original gas in place (Bscf)	13.2	20.7	24.8

The parameters have been ordered to determine three different cases:

1. The minimum case (P10) is 13.2 Bscf;
2. The most probable case (P50) is 20.7 Bscf;
3. The maximum case (P90) is 24.8 Bscf.

The previous promising reserve supports drilling of a new well that could add to hydrocarbon potential for the study area.

The channel thickness is ranging from 12 m to 16 m after delineating upper and lower reservoir. OGIIP is estimated by 20.7 Bscf, which is the most probable case and should be considered for exploration.

Seismic grid was tied with Well-1X well and several reflectors were mapped. Two Way Time and depth maps were generated, in order to investigate the extension of each level. The Pliocene channel has been detected from near and far offset seismic data, as there is the increasing amplitude from near to far data (Fig. 11).

Attribute maps were generated from near and far data sets which showed that the amplitude increased from near to far offset data. RGB could successfully determine the geometry and extension of the Pliocene channel after analysing the amplitude spectrum. The bright green area illustrates the distribution of the channel (Fig. 12).

5. Discussion

Another two studies are performed in West Al-Khilala (*Leila and Moscariello, 2018*) and North West Al-Khilala Field (*Fattah et al., 2022*) (Onshore Nile Delta), which are close to the study area.

The first study (*Leila and Moscariello, 2018*) presents an investigation for the differential impacts of the depositional and petrophysical attributes on the hydrocarbon volumes trapped in the Messinian reservoirs. Analyses of the pressure data and pressure gradients revealed hydraulically-connected and homogeneous Messinian reservoir rocks. The amounts of Stock Tank Oil and Gas Initially in Places are typically controlled by the depositional primary attributes (matrix content and grain size) which induce several reservoir heterogeneities. The volume of gas is increasing with the growing channel width. This is likely due to increasing reservoir connectivity with growing the channel width (*Leila and Moscariello, 2018*).

The main objective of the second study (*Fattah et al., 2022*) is to determine the characteristics of the late Messinian Abu Madi reservoir in the North West Al-Khilala field and study the depletion of the Lower Abu Madi sand interval. This study confirms that there is a production from Abu Madi Formation but there is the depletion due to connection with West Al-Khilala field.

The main difference between the studies and the current study is the focus on shallow reservoir while the above mentioned studies focus on the deep reservoir. Finally, this study and the archive studies agree that the Nile delta is one of the most important and prolific petroleum provinces in Egypt with high hydrocarbon reserve in both shallow and deep reservoirs.

6. Conclusion

Integration of the petrophysical analysis, seismic interpretation and seismic attributes successfully determined the properties and geometry of a Pliocene reservoir channel, located in Disouq Concession (Onshore Nile Delta, Egypt). The petrophysical analysis of Well-1X confirmed the presence of gas and showed that the reservoir consists of three zones: A, B, and C. These zones are characterized by low gamma ray values (around 35%), with relatively high porosity (around 29%) and low water saturation (36–

48%). The reflection seismic grid was tied with the given well. Seismic data are utilized for structural and stratigraphic interpretation. Several horizons are mapped and time as well as depth maps are generated. They showed that the study area is affected by normal fault. The charge enters the channel from the south and the interval is sealed by a shale formation. When comparing the near and far datasets, there was an increase of the negative amplitude from near to far offset data. Spectral decomposition and RGB for far offset data at three frequencies 12, 29, 46 Hz, show the geometry of the channel. The study area is of great economic interest, since it is considered to be a gas prospect with estimated OGIP around 1.13 km³ (in the most probable case). A new well is recommended in the Southern area of the gas channel, which is characterized by low acoustic impedance and four-way dip closure.

Acknowledgements. The author would like to thank the staff of the Exploration Division of the Suez Oil Company for their kind help, for permission to publish the data and for providing the necessary information and facilities to accomplish this work, which is supported by Petrel software. The author would also like to thank the staff of the Geophysics Department, Faculty of Science, and Cairo University for their kind help. The author would also thank the editor and reviewers for accepting and publishing this paper.

References

- Abd-Allah A. M. A., 2008: Mesozoic-Cenozoic inversion tectonic of North Sinai: integration of structural and basin analysis. *J. Appl. Geophys. (Cairo)*, **7**, 77–108.
- Abdel Aal A., Price R. J., Vital J. D., Shallow J. A., 1994: Tectonic evolution of the Nile Delta, its impact on sedimentation and hydrocarbon potential. *Proc. 12th EGPC, Egyptian General Petroleum Corporation Conference, Cairo 1*, 19–34.
- Abdel Aal A., El Barkooky A., Gerrits M., Meyer H.-J., Schwander M., Zaki H., 2001: Tectonic evolution of the Eastern Mediterranean basin and its significance for hydrocarbon prospectivity of the Nile Delta deepwater area. *GeoArabia*, **6**, 3, 363–384, doi: 10.2113/geoarabia0603363.
- Ahmed T., 2010: *Reservoir Engineering Handbook*. Gulf Publishing Company, Houston, Texas, 827–828.
- Archie G. E., 1952: Classification of carbonate reservoir rocks and petrophysical considerations. *AAPG, Am. Assoc. Pet. Geol. Bull.*, **36**, 2, 278–298.
- Brown A. R., 1987: The value of seismic amplitude. *Lead. Edge*, **6**, 10, 30–33, doi: 10.1190/1.1439335.
- Cao J., Yue Y., Zhang K., Yang J., Zhang X., 2015: Subsurface channel detection using color blending of seismic attribute volumes. *Int. J. Signal Process. Image Process.*

- Pattern Recognit., **8**, 12, 157–170, doi: 10.14257/ijssip.2015.8.12.16.
- Dewar J., 2001: Rock physics for the rest of us – An informal discussion. *Can. Soc. Explor. Geophys. Rec.*, **26**, 5, 42–49.
- Dolson J. C., Shann M. V., Matbouly S., Harwood C., Rashed R., Hammouda H., 2001: The petroleum potential of Egypt. In: Downey M. W., Threet J. C., Morgan W. A. (Eds.): *Petroleum Provinces of the Twenty-first Century*. AAPG, Am. Assoc. Pet. Geol. Memoir, **74**, 453–482, doi: 10.1306/M74775C23.
- Fattah N. A., Ibrahim I. M., Elkammar M., 2022: Seismic reservoir characterization and pressure depletion of the Abu Madi Formation in the NW Khilala field, onshore Nile Delta, Egypt. *Contrib. Geophys. Geod.*, **52**, 2, 209–237, doi: 10.31577/congeo.2022.52.2.3.
- Garfunkel Z., 1998: Constrains on the origin and history of the Eastern Mediterranean basin. *Tectonophysics*, **298**, 1-3, 5–35, doi: 10.1016/S0040-1951(98)00176-0.
- Guiraud R., Bosworth W., 1999: Phanerozoic geodynamic evolution of northeastern Africa and northwestern Arabian platform. *Tectonophysics*, **315**, 1-4, 73–108, doi: 10.1016/S0040-1951(99)00293-0.
- Hammond A. L., 1974: Bright spot: Better seismological indicators of gas and oil. *Science*, **185**, 4150, 515–517, doi: 10.1126/science.185.4150.515.
- Harms J. C., Wray J. L., 1990: Nile Delta. In: Said R. (Ed.): *The Geology of Egypt*. Balkema, Rotterdam, 329–344, doi: 10.1201/9780203736678.
- Henderson J., Purves S. J., Leppard C., 2007: Automated delineation of geological elements from 3D seismic data through analysis of multi-channel, volumetric spectral decomposition data. *First Break*, **25**, 3, 87–93, doi: 10.3997/1365-2397.25.1105.27383.
- Henry S. G., 1997: Catch the (seismic) wavelet. *AAPG, Am. Assoc. Pet. Geol. Explor.*, **18**, 3, 36–38.
- Hussein I. M., Abd-Allah A. M. A., 2001: Tectonic evolution of the northeastern part of the African continental margin, Egypt. *J Afr. Earth Sci.*, **33**, 1, 49–68, doi: 10.1016/S0899-5362(01)90090-9.
- Kamel H., Eita T., Sarhan M., 1998: Nile Delta hydrocarbon potentiality. In: *Proc. EGPC, 14th Petroleum Exploration and Production Conference*, **2**, 485–503.
- Kellner A., El Khawaga H., Brink G., Brink-Larsen S., Hesham M., Abu El Saad H., Atef A., Young H., Finlayson B., 2009: Depositional history of the West Nile Delta – Upper Oligocene to Upper Pliocene. Presented at AAPG International Conference and Exhibition, Cape Town, South Africa, October 26-29, 2008, RWE, The energy to Lead, Search and Discovery Article #30092, 25.
- Leila M., Moscariello A., 2018: Depositional and petrophysical controls on the volumes of hydrocarbons trapped in the Messinian reservoirs, onshore Nile Delta, Egypt. *Petroleum*, **4**, 3, 250–267, doi: 10.1016/j.petlm.2018.04.003.
- Moustafa A. R., El-Badrawy R., Gibali H., 1998: Pervasive E-ENE oriented faults in northern Egypt and their effect on the development and inversion of prolific sedimentary basins in the northern Western Desert. In: *Proc. EGPC 14th Exploration and Production Conference*. Cairo, Egypt, 51–67.

- Newton I., 1687: *Philosophiae Naturalis Principia Mathematica*. 510 p. (in Latin).
- Rizzini A., Vezzani F., Cococchetta V., Milad G., 1978: Stratigraphy and sedimentation of a Neogene-Quaternary section in the Nile Delta area (A.R.E.). *Mar. Geol.*, **27**, 3-4, 327–348, doi: 10.1016/0025-3227(78)90038-5.
- Said R., 1990: *The Geology of Egypt*. Balkema, Rotterdam, 10.
- Sarhan M., Hemdan K., 1994: North Nile Delta structural setting and trapping mechanisms, Egypt. 12th EGPC, Egyptian General Petroleum Corporation Conference, Cairo 1, 1–18.
- Sarhan M., Barsoum K., Bertello F., Talaat M., Nobili M., 1996: The Pliocene play in the Mediterranean offshore: structural setting and growth faults controlled hydrocarbon accumulations in the Nile Delta basin. A comparison with the Niger Delta basin. Proc. 13th EGPC, Egyptian General Petroleum Corporation Conference, Cairo 1, 121–139.
- Schlumberger, 1987: *Log interpretation Principles/Applications*. Schlumberger Education Service, Houston, Texas, 69–94.
- Sestini G., 1984: Tectonic and sedimentary history of northeast African margin (Egypt/Libya). In: Dixon J. E., Robertson A. H. F. (Eds.): *The geological evolution of the Eastern Mediterranean*. Geol. Soc. Lond. Spec. Publ., **17**, 161–175.
- Suez, 2014: Final evaluation of well 1X. Suez Oil Co., confidential internal report, 25 p.
- Van Wagoner J. C., Mitchum R. M., Posamentier H. W., Vail P. R., 1987: Seismic stratigraphy interpretation using sequence stratigraphy, Part 2: Key definitions of sequence stratigraphy. In: Bally A. W. (Ed.): *Atlas of Seismic Stratigraphy*. Am. Assoc. Pet. Geol. Stud. Geol., **27**, 1, 11–14.
- Younes M. A.-A., 2015: Natural Gas Geochemistry in the Offshore Nile Delta, Egypt (chapter 2). In: Patel V. (Ed.): *Advances in Petrochemicals*, IntechOpen, 27–31, doi: 10.5772/60575.